Compact bubble clusters in Newtonian and non-Newtonian liquids

J. Rodrigo Vélez-Cordero, Johanna Lantenet, Juan Hernández-Cordero, and Roberto Zenit

Citation: Physics of Fluids (1994-present) **26**, 053101 (2014); doi: 10.1063/1.4874630
View online: http://dx.doi.org/10.1063/1.4874630
View Table of Contents: http://scitation.aip.org/content/aip/journal/pof2/26/5?ver=pdfcov
Published by the AIP Publishing

PHYSICS OF FLUIDS **26**, 053101 (2014)

Compact bubble clusters in Newtonian and non-Newtonian liquids

J. Rodrigo Vélez-Cordero, Johanna Lantenet, Juan Hernández-Cordero, and Roberto Zenit
Instituto de Investigaciones en Materiales, Universidad Nacional Autónoma de México, Apdo. Postal 70-360, México D.F. 04510, Mexico

(Received 22 November 2013; accepted 21 April 2014; published online 5 May 2014)

We studied the terminal velocity of a packed array of bubbles, a bubble cluster, rising in different fluids: a Newtonian fluid, an elastic fluid with nearly constant viscosity (Boger fluid), and a viscoelastic fluid with a shear dependent viscosity, for small but finite Reynolds numbers ($1 \times 10^{-4} < Re < 4$). In all three cases, the cluster velocity increased with the total volume, following the same trend as single bubbles. For the case of clusters in elastic fluids, interestingly, the so-called velocity discontinuity was not observed, unlike the single bubble case. In addition to the absence of jump velocity, the clusters did not show the typical teardrop shape of large bubbles in viscoelastic fluids and the strength of the negative wake is much weaker than the one observed behind single bubbles. Dimensional analysis of the volume-velocity plots allowed us to show that, while the equivalent diameter (obtained from the total cluster volume) is the appropriate length to determine buoyancy forces and characteristic shear rates, the individual bubble size is the appropriate scale to account for surface forces. © *2014 AIP Publishing LLC*. [http://dx.doi.org/10.1063/1.4874630]

I. INTRODUCTION

The rigid character of solid particles has allowed fluid dynamic researchers to find analytical solutions for the motion and interaction of particles in different media.[1–3] Bodies that allow continuity of the velocity at the interface but without retaining stresses on it (vanishing normal and tangential stresses), also constitute classical systems with analytical solutions.[1–3] The complexity of such systems increases if surface deformations are considered, i.e., if normal and tangential stresses are developed at the interfaces. In general, we can expect that interfacial deformability will make bodies behave differently with respect to rigid particles or particles with zero stresses at the surface. For example, Manga and Stone[4] observed that the rate of coalescence in dilute bubble suspensions increases with the Bond number, $Bo = \Delta\rho g r^2/\sigma$, where $\Delta\rho$ is the density difference, g the gravity, r the bubble radius, and σ the surface tension. The Bond number compares buoyancy and surface forces and constitutes a common indicator of surface deformability. It is also thought that interfacial deformability plays a crucial role in the velocity-discontinuity observed in viscoelastic fluids, where the bubble undergoes a change in shape for narrow diameter changes.[5–15]

While single bubbles have been the central model to study the interplay between driving (buoyancy) and restoring (surface tension) forces, little is known regarding the behavior of a group of bubbles rising in a compact array (bubble clusters) with touching interfaces. The motion of particle clusters, in which different interfaces are separated just by a thin liquid film, constitutes a particular case of the general dynamic problem of a group of bodies traveling in a medium having an arbitrary distance between their centers.[1,4,16–22] It is commonly accepted that two particles or bubbles touching each other behave as a single body when moving in a Newtonian fluid. Consider, for example, the velocity relation between a particle with radius r and a particle pair in contact, having the same radius. If we use the convention of defining the equivalent diameter, or radius, of the cluster as the one obtained by summing the individual volumes, considering the pair as a single *bigger* particle, we can compute the terminal velocity of the pair by equating buoyancy

and drag forces, i.e., $2(4/3\pi r^3 g\Delta\rho) = 6\pi\mu U_{II}\sqrt[3]{2}r$, where U_{II} is the velocity of the particle pair and μ is the liquid viscosity. Comparing with the velocity U_I of a single particle, we obtain that $U_I/U_{II} = \sqrt[3]{2}/2 = 0.63$. As expected, the pair travels faster than the individual particle.[21] Analytical solutions for the settling velocity of two particles at low Reynolds numbers having a distance $\delta = l/2r$ between centers are well known in the literature.[1,23] For the case when $\delta = 1$, i.e., touching spheres, Stimson and Jeffery[23] predicted a value of $U_I/U_{II} = 0.645$ for two particles traveling in-line, and a $U_I/U_{II} = 0.707$ was predicted for the case when the particles travel side-by-side.[1] Therefore, in the case where the detailed geometry of the pair and incurrence of relative motion between particles constitute minor effects in the steady velocity, the dynamics of a packed array of particles (cluster) becomes trivial and its solution is equal to the single particle case considering the equivalent diameter d_{eq}.

The main objective of the present work is to investigate if a packed array of bubbles, having any number of bubbles $\mathcal{N}$, obeys, or not, the equivalent diameter rule. Another question that we would like to answer is if bubble clusters in non-Newtonian fluids present the velocity-jump and, ultimately, what is the effect of the buoyancy and surface forces. In order to achieve generality in our results, three different fluids were considered: a Newtonian fluid, an elastic fluid with nearly constant viscosity, and an elastic fluid with a shear-dependent viscosity. Section II presents the experimental setup and the rheological properties of the fluids. Next, the volume-velocity curves are presented in Sec. III together with images of single bubbles and bubble clusters obtained in the experiments. In Sec. IV, we analyze the results considering a dimensionless parameter used as a velocity jump criteria. In Sec. V, the negative wake structure left by a single bubble and a bubble cluster are shown and discussed. Some conclusions are outlined in Sec. VI.

II. EXPERIMENTAL SETUP

A. Bubble column and image processing

Single bubbles and bubble clusters were released in a cylindrical glass tube having an inner diameter of $D = 90$ mm and a length of 75 cm. The ratio of the equivalent diameter of the bubbles (or clusters) with D was in the range of $0.01 < d_{eq}/D < 0.08$ with a mean of 0.043 ± 0.017. As shown in Figure 1, the column is equipped with optic rectifiers, filled with the working fluid, and a bubble dispenser located at the base. This bubble dispenser consist of two concentric glass cylinders with holes at the sidewalls (Figure 1). By moving a flexible straw up and down from the bottom of the column, it is possible to rotate the inner cylinder in order to trap bubbles, feeded by an external tube, or release bubbles inside the column. It is important to note that the bubbles have to be collected and put into contact to conform the cluster before opening the container. If the bubbles are released without previous clustering, they may separate due to the repulsive interaction forces (lubrication forces may also be responsible in preventing bubble separation). Note also that the design of the bubble dispenser allows to form clusters having any bubble size. In principle, we wanted to form clusters with bubbles having a diameter lower than the critical one, V_c, at which the velocity jump occurs. In most of the cases, we succeeded in forming bubbles with nearly the same size, i.e., the total volume of the cluster is proportional to the number of bubbles in it. However, for the cases when the clusters had different bubbles sizes, we calculate the total volume by adding the individual volumes.

Videos of the rising bubbles were taken with a high speed camera (*MotionPro X4*) placed 40 cm from the column base; diffuse illumination was provided by an array of LEDs (*Studio LED Light*). The vertical steady velocity (no lateral displacements were observed) was obtained directly from the image acquisition software package (*Motion Studio 2.07.20*). The equivalent diameter of spherical or ellipsoidal bubbles, including the ones embedded in the clusters, were calculated according to the maximum and minimum diameters formula $d_{eq} = (d_{max}^2 d_{min})^{1/3}$. For teardrop shaped bubbles, the second centroid theorem of Pappus was used to compute the volume V

$$V = 2A\pi r_{centroid}, \tag{1}$$

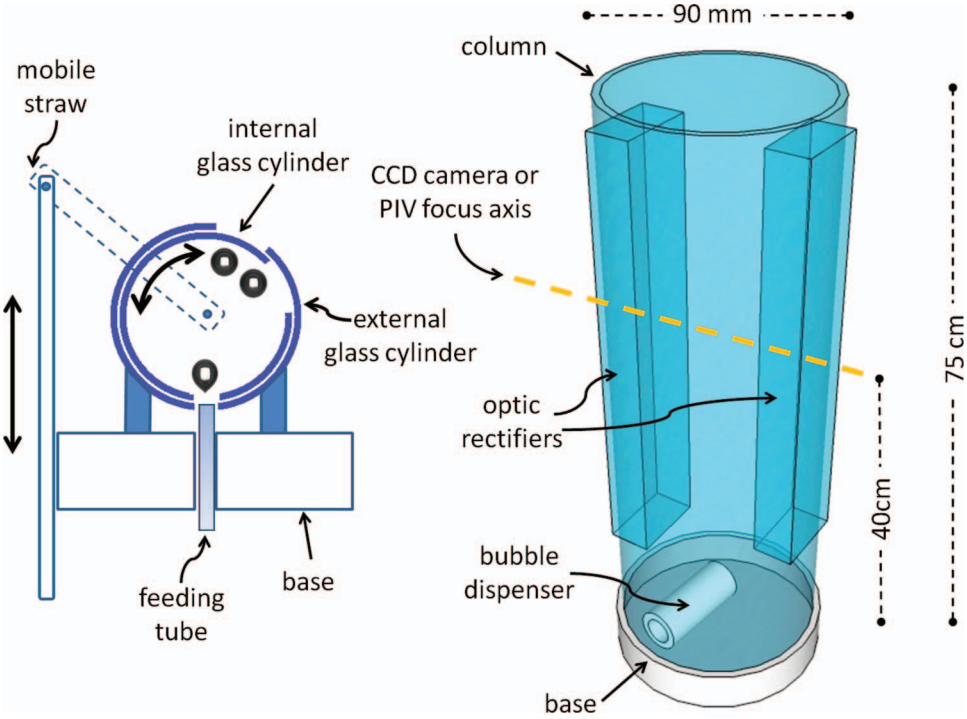

FIG. 1. Experimental setup. Left image: diagram of the bubble dispenser used to collect or release bubbles. A mobile straw is moved up and down from the bottom in order to rotate a glass tube placed inside another cylinder and sealed at the axial sides. Matching the lateral holes between both cylinders allows either bubble trapping or bubble release inside the column. Right image: dimensions of the bubble column. The high speed camera or PIV focusing lenses were placed 40 cm from the bottom facing the front walls of the optic rectifiers.

where A is the half of the projected area of the bubble, considering its axis of symmetry, and $r_{centroid}$ is the length between the axis of symmetry and the centroid of A. The equivalent diameter d_{eq} of the bubbles was then estimated using Eq. (1) and the sphere volume $\pi d_{eq}^3/6$. The image analysis was done with *Matlab*©.

B. Working fluids

In order to form a packed array of bubbles, it is imperative to avoid the rupture of the film separating the individual bubbles, i.e., avoid bubble coalescence. Therefore, all the fluids need to have a viscosity such that the thin film separating the bubbles becomes stable at least during the rising time of the bubbles in the column. Taking into account this consideration, for the Newtonian fluid we used pure glycerin ($\mu = 692.1$ mPa s at 25 °C). The elastic fluid with nearly constant viscosity (Boger-type fluid) was made by dissolving 1.5% of HASE polymer (*Primal TT-935*, supplied by Rohm and Haas) in water adjusting the pH to 9.0 with a 0.1M solution of 2-amino-2-methyl-1-propanol. Finally, the viscoelastic fluid was prepared by mixing 0.13% w/w of polyacrylamide (Paam, *Separan AP-30*) in a 50/50 water-glycerin mixture. The viscosity and first normal stress difference (N_1) of the fluids are shown in Figure 2. The rheological measurements were done in a *TA Instruments* rheometer (AR1000N, cone-plate geometry 60 mm, 1°) at 25 °C.

The viscosity of the Paam solution can be fitted to the power-law model having $k = 0.87$ Pa s^n and $n = 0.478$; while the viscosity of the Boger-type fluid was modeled with the Carreau equation having $\mu_o = 2.014$ Pa s, $\lambda_t = 0.0716$ s^{-1}, and $n = 0.618$. Also note that in the shear-rate range found in the experiments, denoted by the vertical dashed lines in Figure 2, N_1 is larger in the viscoelastic fluid than in the Boger-type fluid (actually, no normal stress differences were registered by the rheometer for the latter for $\dot{\gamma} < 16$ s^{-1}). Evidently, for larger values of $\dot{\gamma}$, the HASE fluid becomes more elastic. Considering that $Wi \sim N_1(\dot{\gamma})/\mu(\dot{\gamma})\dot{\gamma}$, we estimated for the Paam solution a

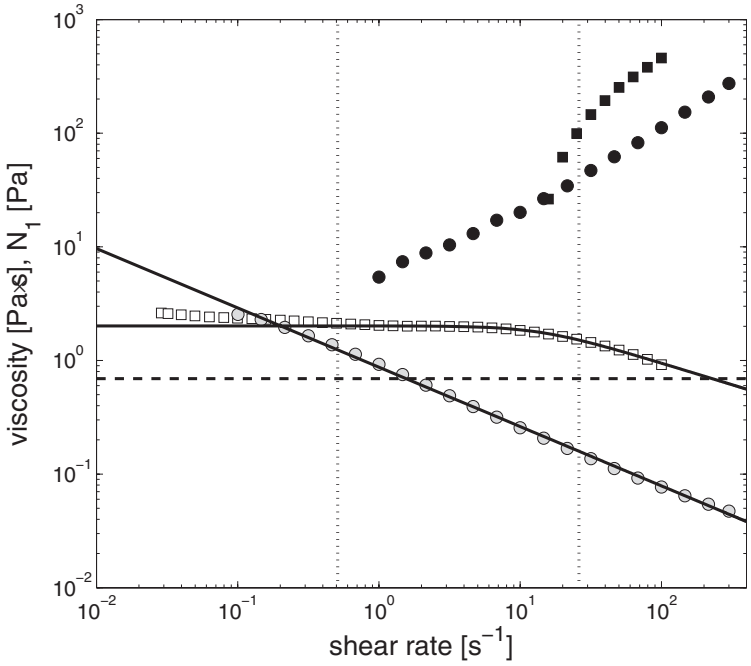

FIG. 2. Rheological properties of the fluids. The dashed horizontal line denotes the viscosity of the Newtonian fluid; (○) symbols are for the viscoelastic fluid, and (□) symbols are for the Boger fluid; empty symbols indicate the values of the viscosity, μ, and filled symbols the values of the first normal stress difference N_1. The vertical dashed lines denote the shear rate range ($0.51 < \dot{\gamma} < 26.03$) calculated from the experiments. The solid lines denote model fittings for the viscosity, the power law model $\mu = 0.8714\dot{\gamma}^{0.478-1}$ for the viscoelastic fluid, and the Carreau model $\mu = 2.014[1 + (0.0716\dot{\gamma})^2]^{(0.618-1)/2}$ for the Boger-type fluid.

Weissenberg number range of $5.7 < Wi < 9.2$. In the case of the HASE fluid, we can consider a Weissenberg number of the order of $Wi \sim \lambda_t \dot{\gamma}$,[24] giving a range of $0.04 < Wi < 0.6$.

III. VOLUME-VELOCITY CURVES FOR SINGLE BUBBLES AND BUBBLE CLUSTERS

The images of single bubbles and bubble clusters released in the column are shown in Fig. 3 for the three fluids. The volume-velocity plots are shown in Figs. 4–6 for the Newtonian, Boger, and viscoelastic fluids, respectively. In all cases, the experimental velocity values were compared with the theoretical values (lines in the volume-velocity plots) using the formula for a generalized Newtonian fluid in the creeping flow regime[3]

$$U = \left[\frac{\Delta\rho g r_{eq}^{n+1}}{kY(n)}\right]^{1/n}, \tag{2}$$

where we have assumed *a priori* that clusters obey the equivalent diameter rule. The drag correction factor $Y(n)$ for rigid spheres is considered as[25]

$$Y(n)_{rigid} = \frac{9}{2^n} 3^{\frac{3n-3}{2}} \left[\frac{2 + 29n - 22n^2}{n(n+2)(2n+1)}\right], \tag{3}$$

while the drag correction factor for mobile interfaces was considered as[26]

$$Y(n)_{mobile} = 3^{\frac{n+1}{2}} \left[\frac{13 + 4n - 8n^2}{(n+2)(2n+1)}\right]. \tag{4}$$

The reported Reynolds numbers were computed as

$$Re = \left(2^{1-n}\right) \frac{\rho U^{2-n} d_{eq}^n}{k}. \tag{5}$$

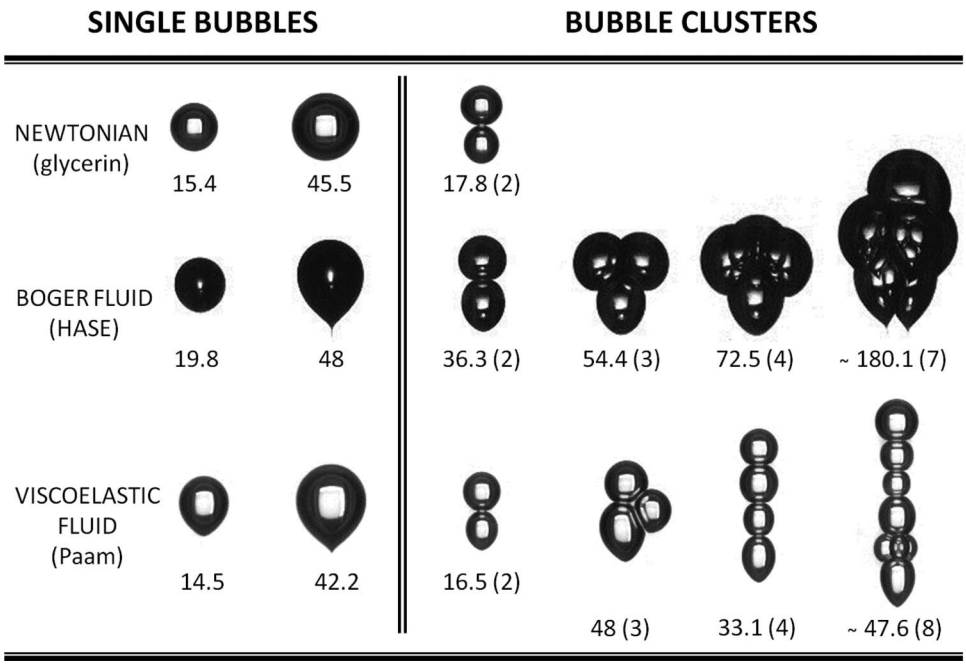

FIG. 3. Images of single bubbles and bubble clusters formed in the three fluids considered in this work. The numbers below each image indicate the bubble (or cluster) volume [mm^3], and the numbers in parenthesis indicate the number of bubbles forming the cluster.

The factor 2^{1-n} is usually dropped from this expression, but we retained it in this case to be consistent with the characteristic lengths disclosed below.

At a first glance, we can see that single bubbles and bubble clusters follow closely, in the three fluids, the solution for spheres (generalized Stokes solution) in the creeping flow regime,

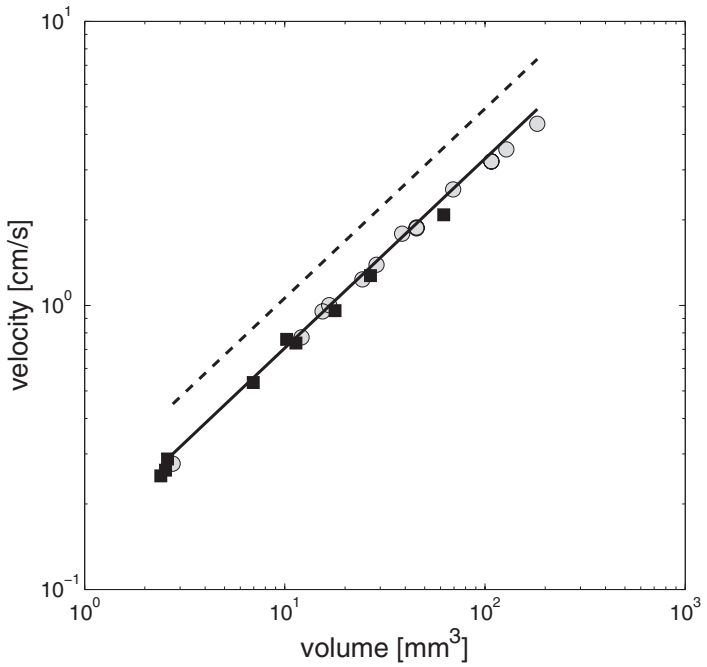

FIG. 4. Experimental velocity values for single bubbles (gray circles) and bubble clusters (■) obtained for the Newtonian fluid. The lines are the theoretical values according to Eq. (2) using Eq. (3) for rigid spheres (thick line) or Eq. (4) for mobile interfaces (dashed line) having $n = 1$.

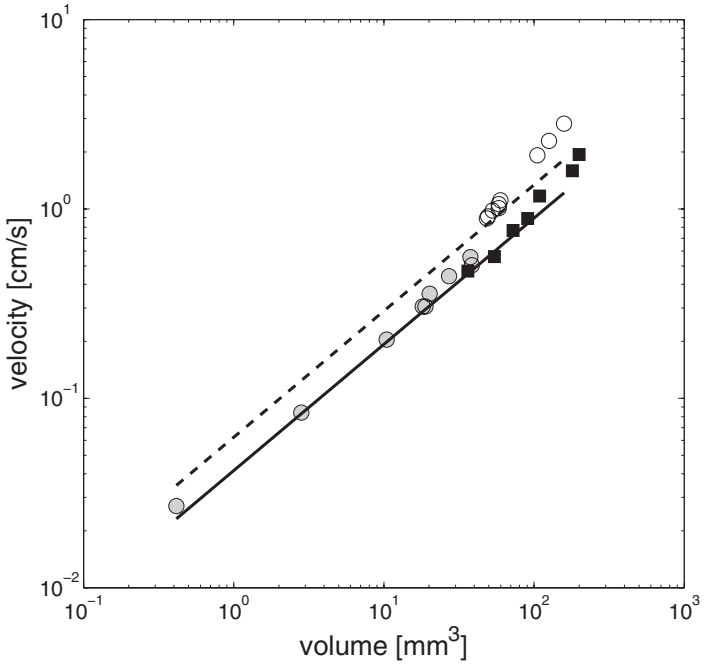

FIG. 5. Experimental velocity values for single bubbles having $V < V_c$ (gray circles), single bubbles having $V > V_c$ (○), and bubble clusters (■) obtained for the Boger (HASE) fluid. The lines are the theoretical values according to Eq. (2) using Eq. (3) for rigid spheres (thick line) or Eq. (4) for mobile interfaces (dashed line) having $n = 1$ ($\mu_o = 2.014$ mPa s). The critical volume is $V_c = 43$ mm^3.

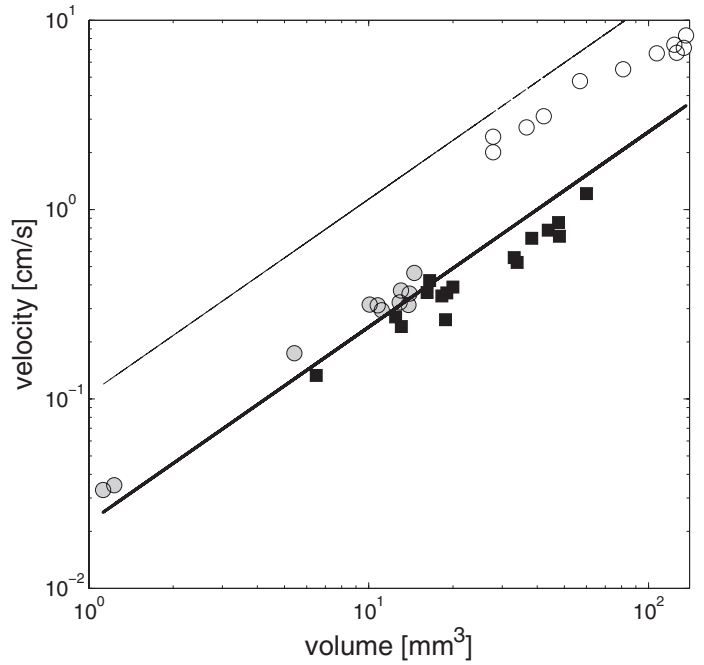

FIG. 6. Experimental velocity values for single bubbles having $V < V_c$ (gray circles), single bubbles having $V > V_c$ (○), and bubble clusters (■) obtained for the viscoelastic (Paam) fluid. The lines are the theoretical values according to Eq. (2) using Eq. (3) for rigid spheres (thick line) or Eq. (4) for mobile interfaces (thin line) having $n = 0.478$ and $\mu_{ref} = k = 0.87$ Pa s^n. The critical volume is $V_c = 21$ mm^3.

indicating that the inertia and wall effects are small. For the two elastic fluids, however, single bubbles experience the velocity jump at the critical volume V_c, while the bubbles clusters do not show velocity discontinuity. In all cases, some bubble movement within the cluster and cluster rearrangement was observed immediately after release. After this initial adjustment, we did not observe relative motion within the cluster or cluster rotation along the measurement site (40 cm above the release point). We proceed now with the phenomenological description for each fluid.

The Newtonian case (Figure 4) reveals that the equivalent diameter rule is obeyed in simple fluids: touching bubbles can be considered single bubbles with an equivalent diameter d_{eq}, at least for the cases where the bubbles *do not* move relative to one another during the rising motion and when the fluid is inelastic. Moreover, the particular geometry of the bubble clusters (in our case, a kind of "8" shape, see Figure 3) do not introduce additional drag, and single bubbles and bubble clusters behave as rigid particles (see Figure 4). As expected, the single bubble shape is almost spherical due to small inertia and buoyancy forces with respect to viscous and surface forces (maximum Reynolds and Eötvös numbers, $Eo = g\Delta\rho d_{eq}^2/\sigma$, were 0.55 and 10, respectively, considering a surface tension of $\sigma = 63$ mN/m). In this fluid, we could only form bubble pairs (see Figure 3) varying the size of the individual bubbles; clusters formed with more than two bubbles disaggregate into smaller clusters.

For the Boger fluid, shown in Figure 5, the single bubble velocity increases with the volume as in the case for Newtonian liquids, but at a critical volume ($V_c = 43$ mm^3) the velocity suddenly increases. The single bubbles follow closely the theoretical predictions of solid spheres if the volume is below the critical one; for bubbles with larger volumes, the experimental velocities are closer to the prediction for particles with a slip interface (clean bubbles). The magnitude of the velocity jump at V_c is $U_{after}/U_{before} = 1.76$, close to the Stokes-Hadamard velocity ratio (1.5). Interestingly, the velocity of bubble clusters do not experience velocity jump and its value remains close to that for rigid particles. This indicates that the bubble clusters are insensitive to the elastic stresses developing in the fluid which promotes the velocity jump in single bubbles. The theoretical lines in Figure 5 were calculated considering a Newtonian behavior in the shear-rate range. The approximate expression proposed by Machač *et al.*[27] for Carreau fluids practically followed the Stokes solution after substituting the Carreau parameters obtained in the rheometer. In this fluid, we could form clusters with different number of bubbles, each individual bubble having a $V < V_c$: from two to seven bubbles and a very irregular cluster formed with ∼11 bubbles, all denoted by square symbols in Figure 5; some cluster images are shown in Figure 3 (see also Ref. 28). In addition to missing the velocity jump, clusters formed with 2, 3, and 4 bubbles do not deform as the single bubbles, which experience surface deformation at the rear end (teardrop shape) for $V > V_c$. Note also that clusters made with more than 4 bubbles present deformation in just one or two bubbles at the tail (see Figure 3). An interesting observation, which is linked to this behavior, is that while the clusters do not present a velocity jump at V_c, Figure 5 suggest that they may experience a *gradual* change from no-slip to slip condition. Finally, the Boger fluid confirms that the equivalent diameter rule is obeyed for any number of bubbles forming a cluster at least for the cases when the cluster does not disaggregate in smaller ones.

The behavior of the viscoelastic fluid (Paam solution, Figure 6) is, in general, similar to the Boger fluid: single bubbles having $V < V_c$ ($V_c = 21$ mm^3) and bubble clusters behave as rigid particles, while single bubbles with $V > V_c$ behave as stress-free bubbles. Unlike the previous case, however, none of the bubble clusters showed a cusped tail (Figure 3), and the experimental points for the clusters (square symbols in Figure 6) follow the generalized Stokes solution. Actually, a slight decrease of the rise velocity is observed for the clusters compared with the single bubble trend and the theoretical line. Such velocity decrease, which corresponds to an increase of about 20% of the drag correction factor, suggests that additional elastic stresses act over the bubble interfaces forming the clusters. The normal stress differences shown in the rheological data (Figure 2) together with the Wi numbers calculated for this fluid, and the shape of the clusters, which show bubble chaining with an evident larger aspect ratio with respect to single bubbles (maximum to minimum diameter ratio, see Figure 3), support this observation. In spite of this, again, the elastic stresses forming in the fluid do not favor a velocity jump in the cluster. Finally, the experimental velocity increment

is $U_{after}/U_{before} = 4.33$. The theoretical value for a generalized Newtonian fluid can be computed according to $U_{mobile}/U_{rigid} = [Y(n)_{rigid}/Y(n)_{mobile}]^{1/n}$,[3] which, after using Eqs. (3) and (4) and the value of $n = 0.478$ gives 4.73, i.e., the interface in single bubbles indeed experience mobilization, which is not the case in the bubble clusters.

IV. BUOYANCY AND SURFACE FORCES ACTING IN BUBBLE CLUSTERS

As mentioned above, the theoretical values of the rise velocity were determined using Eq. (2), which is derived from the balance between buoyancy and drag forces considering the equivalent radius (or d_{eq}). Agreement with the experimental data confirmed the straightforward assumption that each bubble contributes to the sum of the total buoyancy force, and, in general, to the cross-sectional area related to the drag force. The contribution of the individual bubbles to the total surface is, however, not additive, and the clusters can be considered as single bodies having a "segmented" interface; in other words, there is no such "equivalent surface." The reason of this is because the radius of curvature linked to the surface tension is approximately equal to the radius of the individual bubbles (r_{ind}) and not to the equivalent radius of the cluster itself. In order to test this asseveration, we computed a dimensionless number used to predict V_c, which considers the surface stresses σ/r. In this manner, we can determine if single bubbles and bubble clusters form a single master curve for the velocity jump criteria. Among the different dimensionless numbers that have been proposed to predict V_c, the parameter α, proposed by Ref. 11 is defined as

$$\alpha = \Pi Ca = \left(\frac{N_1 r}{\sigma}\right)\left(\frac{\mu U}{\Delta\sigma}\right). \tag{6}$$

The parameter α states that the velocity jump occurs when $\alpha = 1$. The term $\frac{N_1}{\sigma/r}$ is a balance between elastic and surface stresses, intuitively needed to produce bubble deformation at the rear end; on the other hand, the modified Capillary number $Ca = \mu U/\Delta\sigma$ is the balance between viscous ($\sim\mu U/r$) and Marangoni stresses ($\sim\Delta\sigma/r$, $\Delta\sigma$ being the difference between the surface tension of the solvent and that of the polymeric solution) involved in the tangential motion of the interface and subsequent mobilization of surfactants acting on it.[10] For our purposes, i.e., considering single bubbles and bubble clusters, we must compute α as

$$\alpha = \left[\frac{N_1(\dot\gamma) r_{ind}}{\sigma}\right]\left[\frac{\mu(\dot\gamma) U}{\Delta\sigma}\right], \tag{7}$$

where $\dot\gamma = 2U/d_{eq}$. The plot of U/U_{rigid} as a function of the parameter α is shown in Figure 7 for the case of the Paam solution, where all the rheological information is available to compute $N_1(\dot\gamma)$ and $\mu(\dot\gamma)$. A value of $\sigma = 66$ mN/m and $\Delta\sigma = 3$ mN/m were considered using the experimental data of Ref. 12 for a 0.15% w/w Paam solution in 50/50 water-glycerin mixture. As shown in the figure, single bubbles and bubble clusters with $V < V_c$ have a value of $\alpha < 1$ (no velocity jump prediction), as expected. On the contrary, single bubbles with $V > V_c$ have a value $\alpha > 1$, while bubble clusters still have a value less than one. This observation is important in two ways: confirms that bubble clusters resist deformation due to the fact that the effective curvature is related to $1/r_{ind}$ rather than $1/r_{eq}$; indirectly, this also supports the idea that interfacial deformability is important for the velocity jump to occur.

V. NEGATIVE WAKE BEHIND SINGLE BUBBLES AND BUBBLE CLUSTERS

In order to close our discussion on the difference between single bubble and bubble clusters, we studied the flow structure formed in both cases, particularly in the region behind the bubbles where the negative wake appears. We conducted PIV measurements for the HASE fluid, whose extensional properties promote the formation of a negative wake behind particles or bubbles.[8,29] Differences in the negative wake structure or extensional properties between the HASE and Paam solutions are out of the scope of the present investigation; some information in this regard can be found in

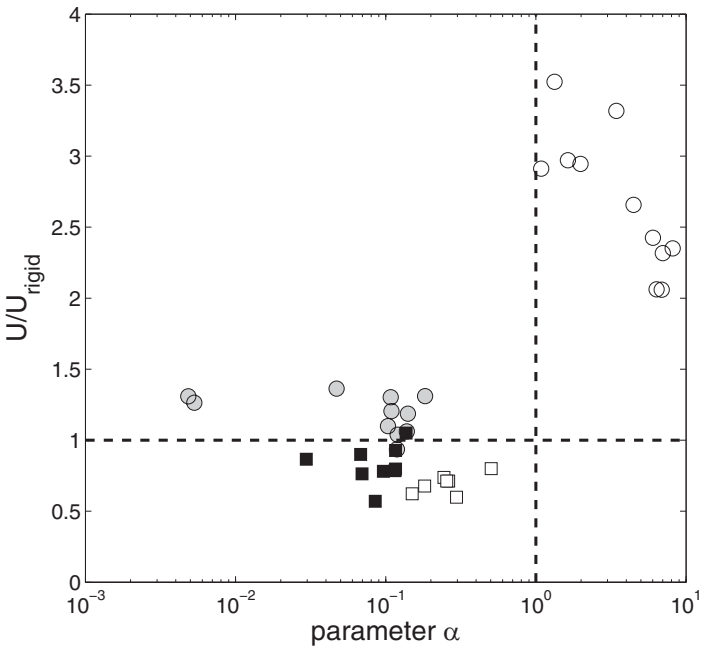

FIG. 7. Map of the experimental rise velocity U, normalized by the generalized Stokes velocity U_{rigid} (Eqs. (2) and (3)), as a function of the parameter α computed for the viscoelastic (Paam) fluid. Single bubbles having $V < V_c$: gray circles, bubble clusters having $V < V_c$ (■), single bubbles having $V > V_c$ (○), bubble clusters having $V > V_c$ (□). The horizontal and vertical dashed lines denote the values $U/U_{rigid} = 1$ and $\alpha = 1$.

Refs. 29 and 30. Figure 8 shows instantaneous velocity fields left by a single bubble ($V = 194$ mm^3) and a bubble cluster ($V \approx 240$ mm^3, formed by ~11 bubbles). Note that in both situations the volume is larger that the critical one ($V_c = 43$ mm^3). For the single bubble case, a negative wake is evidently formed at $y/r \approx 7$ away from the bubble center and extends beyond $y/r = 20$. On the contrary, a very mild negative wake seems to develop behind the cluster at $y/r \approx 16$. Consistent with the assumption that bubble clusters behave as rigid bodies and resist surface deformation, the appearance of the negative wake in this case is not related with a sudden change on the surface geometry of the bubble, as seen in single bubbles,[9] but it seems to depend just on the extensional properties of the fluid, as is in the case of settling particles.[29,31]

The conjunction of all these observations leads us to consider a non-linear scenario, i.e., an information feedback between the liquid and the interface: the gradual increase of the extensional deformation affects the particle motion; in turn, the particle may adapt or not to such flow, affecting the fluid structure at the downstream flow. Hence, it seems reasonable to consider that deformable bodies can adapt to the extensional flow and promote an early formation of a negative wake near the particle. To our knowledge, no comparative study exists in the literature regarding the differences in the wake structure between rigid and deformable bodies having similar buoyancy forces. This work is the first attempt to conduct this comparison and the results suggest that the cusped-end shape of the bubbles, with possible surface mobility, speed up the relaxation of polymer molecules downstream. The evidence that particle deformability intervenes in the formation of the negative wake does not contradict the conclusions of Kemiha *et al.*,[32] which stated that the rheological behavior of the liquid is essentially the one that causes its appearance. Hence, the present discussion does not change the current understanding of the appearance of the negative wake. In turn, our results can be used to understand finer aspects of the strength of the wake. In a future investigation, we plan to further analyze the influence of having a deformable surface on the shape of the wake and the position of the stagnation point.

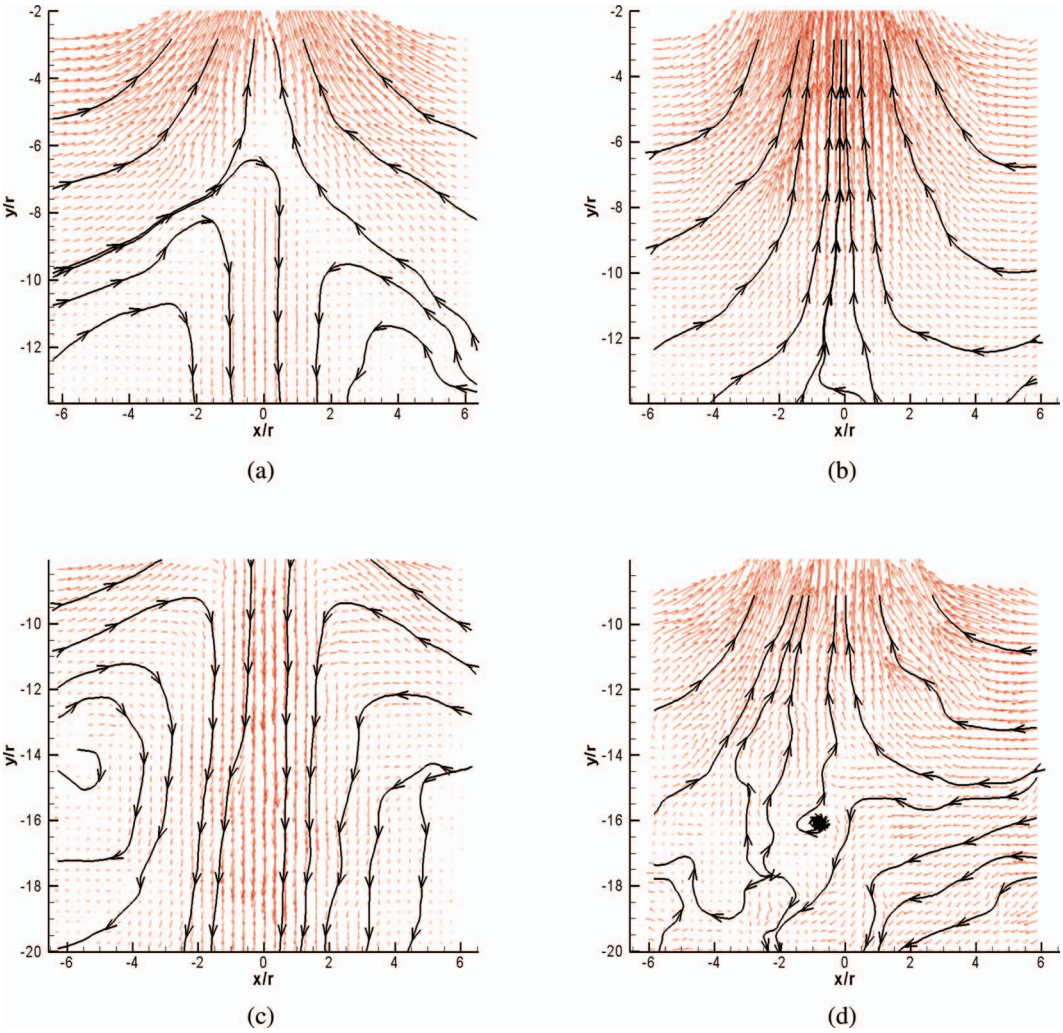

FIG. 8. Velocity field obtained by PIV in the Boger (HASE) fluid of the wake left by the passage of a single bubble or a bubble cluster having both a volume above the critical one. Single bubble ($V = 194$ mm^3): (a) $-14 < y/r < -2$, (c) $-20 < y/r < -8$; bubble cluster ($\mathcal{N} \sim 11$, $V \approx 240$ mm^3): (b) $-14 < y/r < -2$, (d) $-20 < y/r < -8$. The lines show some of the streamlines. The center of the bubble or the cluster is located at (0,0). The grid coordinates were normalized by the bubble radius or the equivalent cluster radius.

VI. CONCLUSIONS

In this investigation, we found that a compact array of non-coalescing bubbles behave as single bubbles and that the calculation of the equivalent diameter is enough to explain with limited accuracy their rise velocity in Newtonian fluids, elastic fluids with nearly constant viscosity, and in viscoelastic fluids. On the other hand, we also found that bubble clusters do not experience the velocity jump discontinuity seen in single bubbles; instead, they shift to the free-interface condition in a gradual manner in cases where some of the bubbles composing the cluster experience deformation (teardrop shape). Using a velocity jump criteria that considers the equivalent diameter for stress computation, but the individual radii of the bubbles to calculate the surface stresses, we found that single bubbles previous to the velocity jump and bubble clusters fall in a single master curve, in which the criteria parameter do not predict a velocity jump. This led us to rationalize the bubble cluster as a single bubble having a "segmented surface" that resists deformation (the surface immobilization works at the scale of the single bubbles forming the cluster). Outstandingly, this confirms experimentally that surface deformation and changes on the boundary conditions are necessary for the velocity

jump appearance. Furthermore, PIV measurements allowed us to observe differences between the negative wake formed behind a single bubble and that formed behind bubble clusters having both a volume above the critical one and similar buoyancy forces. While the single bubble left a very robust negative wake that extends beyond 20 bubble radii, a negative wake is barely visible for the case of the bubble cluster. This demonstrates that the dependence between fluid flow (shear and extensional) and boundary conditions (including surface geometry) goes in both senses: fluid flow affects the motion of the particle, but, in turn, the particle can become adapted or not to the flow influencing the latter as well.

ACKNOWLEDGMENTS

J.R. Vélez-Cordero acknowledges the postdoctoral support of CONACyT-México under Grant No. 154464.

[1] J. Happel and H. Brenner, *Low Reynolds Number Hydrodynamics* (Kluwer Academic Publishers, Netherlands, 1991).
[2] R. Clift, J. R. Grace, and M. E. Weber, *Bubbles, Drops and Particles* (Dover Publications, USA, 2005).
[3] R. P. Chhabra, *Bubbles, Drops and Particles in Non-Newtonian Fluids*, 2nd ed. (Taylor & Francis, USA, 2007).
[4] M. Manga and H. A. Stone, "Collective hydrodynamics of deformable drops and bubbles in dilute low Reynolds number suspensions," J. Fluid Mech. **300**, 231 (1995).
[5] J. R. Vélez-Cordero, D. Sámano, and R. Zenit, "Study of the properties of bubbly flows in Boger-type fluids," J. Non-Newtonian Fluid Mech. **175**, 1 (2012).
[6] C. Pilz and G. Brenn, "On the critical bubble volume at the rise velocity jump discontinuity in viscoelastic liquids," J. Non-Newtonian Fluid Mech. **145**, 124 (2007).
[7] S. B. Pillapakkam, P. Singh, D. Blackmore, and D. Aubry, "Transient and steady state of rising bubble in a viscoelastic fluid," J. Fluid Mech. **589**, 215 (2007).
[8] E. Soto, C. Goujon, R. Zenit, and O. Manero, "A study of velocity discontinuity for single air bubbles rising in an associative polymer," Phys. Fluids **18**, 121510 (2006).
[9] J. R. Herrera-Velarde, R. Zenit, D. Chehata, and B. Mena, "The flow of non-Newtonian fluids around bubbles and its connection to the jump discontinuity," J. Non-Newtonian Fluid Mech. **111**, 199 (2003).
[10] D. Rodrigue and D. De Kee, in *Recent Developments in the Bubble Velocity Jump Discontinuity, in Transport Processes in Bubble, Drops, and Particles*, 2nd ed., edited by D. De Kee and R. P. Chhabra (Taylor & Francis, NY, 2002).
[11] D. Rodrigue, D. De Kee, and C. F. Chan Man Fong, "Bubble velocities: Further developments on the jump discontinuity," J. Non-Newtonian Fluid Mech. **79**, 45 (1998).
[12] D. Rodrigue, D. De Kee, and C. F. Chan Man Fong, "An experimental study of the effect of surfactants on the free rise velocity of gas bubbles," J. Non-Newtonian Fluid Mech. **66**, 213 (1996).
[13] Y. J. Liu, T. Y. Liao, and D. D. Joseph, "A two-dimensional cusp at the trailing edge of an air bubble rising in a viscoelastic liquid," J. Fluid Mech. **304**, 321 (1995).
[14] A. Acharya, R. A. Mashelkar, and J. Ulbrecht, "Mechanics of bubble motion and deformation in non-Newtonian media," Chem. Eng. Sci. **32**, 863 (1977).
[15] G. Astarita and G. Apuzzo, "Motion of gas bubbles in non-Newtonian liquids," AIChE J. **11**, 815 (1965).
[16] Y. Hallez and D. Legendre, "Interaction between two spherical bubbles rising in a viscous liquid," J. Fluid Mech. **673**, 406 (2011).
[17] D. Legendre, J. Magnaudet, and G. Mougin, "Hydrodynamic interactions between two spherical bubbles rising side by side in a viscous liquid," J. Fluid Mech. **497**, 133 (2003).
[18] J. Zhang and L.-S. Fan, "On the rise velocity of an interactive bubble in liquids," Chem. Eng. J. **92**, 169 (2003).
[19] S.-C. Liang, T. Hong, and L.-S. Fan, "Effects of particle arrangements on the drag force of a particle in the intermediate flow regime," Int. J. Multiphase Flow **22**, 285 (1996).
[20] H. Yuan and A. Prosperetti, "On the in-line motion of two spherical bubbles in a viscous fluid," J. Fluid Mech. **278**, 325 (1994).
[21] K. O. L. F. Jayaweera, B. J. Mason, and G. W. Slack, "The behavior of cluster of spheres falling in a viscous fluid," J. Fluid Mech. **20**, 121 (1964).
[22] L. M. Hocking, "The behavior of clusters of spheres falling in a viscous fluid," J. Fluid Mech. **20**, 129 (1964).
[23] M. Stimson and G. B. Jeffery, "The motion of two spheres in a viscous fluid," Proc. R. Soc. **A111**, 110 (1926).
[24] M. M. Cross, "Relation between viscoelasticity and shear-thinning behaviour in liquids," Rheol. Acta **18**, 609 (1979).
[25] Y. Kawase and J. J. Ulbrecht, "Drag and mass transfer in non-Newtonian flows through multi-particle systems at low Reynolds numbers," Chem. Eng. Sci. **36**, 1193 (1981).
[26] T. Hirose and M. Moo-Young, "Bubble drag and mass transfer in non-Newtonian fluids: Creeping flow with power-law fluids," Can. J. Chem. Eng. **47**, 265 (1969).
[27] I. Machač, B. Šiška, and L. Machačová, "Terminal falling velocity of spherical particles moving through a Carreau model fluid," Chem. Eng. Process. **39**, 365 (2000).
[28] J. R. Vélez-Cordero, D. Sámano, and R. Zenit, "Bubble clusters in associative polymers. Part VII. Gallery of fluids," in *Experimental and Theoretical Advances in Fluid Dynamics*, edited by J. Klapp *et al.* (Springer-Verlag, Berlin, 2012).

[29] A. J. Mendoza-Fuentes, R. Montiel, R. Zenit, and O. Manero, "On the flow of associative polymers past a sphere: Evaluation of negative wake criteria," Phys. Fluids **21**, 033104 (2009).
[30] E. Pelletier, C. Viebke, J. Meadows, and P. A. Williams, "Dilute polyacrylamide solutions under uniaxial extensional flow," Langmuir **19**, 559 (2003).
[31] H. S. Dou and N. Phan-Thien, "Criteria of negative wake generation behind a cylinder," Rheol. Acta **43**, 203 (2004).
[32] M. Kemiha, X. Frank, S. Poncin, and H. Z. Li, "Origin of the negative wake behind a bubble rising in non-Newtonian fluids," Chem. Eng. Sci. **61**, 4041 (2006).